九州大学学術情報リポジトリ Kyushu University Institutional Repository

Maximum observable thickness of 4H-SiC crystals by high-voltage scanning transmission electron microscopy

Sato, Kazuhisa

Research Center for Ultra-High Voltage Electron Microscopy, The University of Osaka

Hosono, Kotaro

Division of Materials and Manufacturing Science, Graduate School of Engineering, The University of Osaka

Takagi, Shunya

Research Center for Ultra-High Voltage Electron Microscopy, The University of Osaka

https://hdl.handle.net/2324/7391579

出版情報: Materials Letters. 402, pp.139310-, 2025-08-14. Elsevier BV

バージョン:

権利関係: © 2025 The Authors. Published by Elsevier B.V.



ELSEVIER

Contents lists available at ScienceDirect

Materials Letters

journal homepage: www.elsevier.com/locate/matlet



Maximum observable thickness of 4H-SiC crystals by high-voltage scanning transmission electron microscopy

Kazuhisa Sato^{a,*}, Kotaro Hosono^b, Shunya Takagi^a

- a Research Center for Ultra-High Voltage Electron Microscopy, The University of Osaka, 7-1 Mihogaoka, Ibaraki 567-0047 Osaka, Japan
- b Division of Materials and Manufacturing Science, Graduate School of Engineering, The University of Osaka, 2-1 Yamadaoka, Suita 565-0871 Japan

ARTICLE INFO

Keywords:
High-voltage electron microscopy
Observable thickness
Power device
Dislocation
Top-bottom effect

ABSTRACT

An experimental method has been demonstrated to evaluate dislocations in 4H-SiC crystals that affect the performance of industrially important power devices. Using high-voltage electron microscopy with 1 MeV electrons, it is possible to visualize dislocations contained in a 5 μ m-thick crystal with a spatial resolution of \sim 10 nm. This method has a 10^3 times better spatial resolution than currently existing characterization methods for crystalline defects in semiconductor wafers. Scanning transmission electron microscopy (STEM) is suitable for imaging thick specimens than transmission electron microscopy (TEM) in respect of image blurring due to chromatic aberration caused by inelastic scattering of electrons with increasing specimen thickness. With the proposed method, the maximum observable specimen thickness was determined to be 8.6 μ m for STEM and 5.4 μ m for TEM.

1. Introduction

Highly energy-efficient semiconductor power devices are used in a wide range of applications, including electric vehicles, railway vehicles, and renewable energy systems. Silicon carbide (SiC) is a promising candidate for high-voltage and low-loss power devices [1]. Since the electrical properties of this material are degraded by crystal defects, especially dislocations, it is important to evaluate the dislocations as well as to reduce the dislocation density. To detect and characterize dislocations, transmission electron microscopy (TEM) is useful in respect of spatial resolution compared to other techniques that cover a macroscopic range [2,3]. A limitation of conventional TEM is that, in exchange for high spatial resolution, the observable specimen thickness is limited to ~ 100 nm. It should be emphasized here that the importance of observing sufficiently thick specimens that can be regarded as bulk is especially true for characterization of dislocations by TEM. This is because dislocations may disappear from the surface of a thin specimen for TEM [4]. To this end, we have recently demonstrated the utility of high-voltage electron microscopy (HVEM) in scanning transmission mode (STEM) for visualizing threading dislocations in GaN crystals [5]. The aim of this study is to evaluate the maximum specimen thickness of 4H-SiC crystals observable by HVEM, based on the width of dislocation images as a measure for visibility.

High-density dislocations were artificially introduced into a commercially available 4H-SiC single crystal wafer (N-type, New Metals and Chemicals Corporation) via indentation at room temperature using a Vickers hardness tester (Shimadzu HMV-G20, load: 2 kg, dwell time: 2 s) followed by annealing at 1173 K for 600 s in a high-vacuum furnace (crystal structure is shown in Supplementary Fig. 1S). Wedge-shaped specimens were cut from an area in the vicinity of a crack caused by the indentation using a focused ion beam system (Thermo Fisher Scientific Scios2 Dual Beam). The specimen shapes were characterized by scanning electron microscopy (SEM). The dislocations were observed by HVEM (JEOL JEM-1000EES) operated at 1 MV. We subjected the specimen to a two-beam condition by exciting 11 $\overline{2}$ 0 reflection of 4H-SiC. In the bright-field (BF) STEM imaging, the beam convergence was set to a semiangle of 3.75 mrad and the outer collection semiangle of 13 mrad. BF-TEM images were acquired with an aperture angle of 2.3 mrad.

3. Results and discussion

Fig. 1(a) shows a secondary electron image of a cross-section of a wedge-shaped 4H-SiC crystal. As can be seen, the cross-sectional shape is an isosceles triangle with a 20.5° apex angle, a base length of $5.9 \, \mu m$, and a height of $16.8 \, \mu m$. In the subsequent HVEM observations,

E-mail address: sato@uhvem.osaka-u.ac.jp (K. Sato).

^{2.} Materials and methods

^{*} Corresponding author.

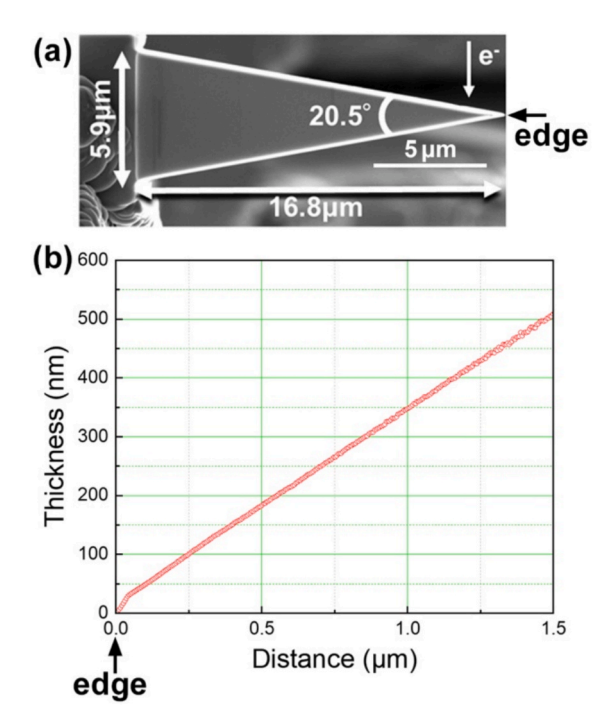


Fig. 1. (a) SEM image of a wedge-shaped 4H-SiC crystal. (b) The relationship between specimen thickness and distance from the edge of the specimen.

electrons are incident in the direction indicated by a vertical arrow in the figure, so the base length corresponds to the maximum specimen thickness for TEM. As will be described later, we prepared wedge-shaped samples with different apex angles (see Supplementary Fig. 2S). Referring to Fig. 1(a), the distance from the apex (i.e., one of the edges of the specimen indicated by an arrow) determines the thickness of the specimen at that location. We used electron energy-loss spectroscopy (EELS) to measure the specimen thickness near the specimen edge more precisely. Fig. 1(b) shows the specimen thickness versus the distance from the specimen edge. An almost linear relationship was obtained except in the immediate vicinity of the specimen edge. Here, the specimen thickness was calculated using $\lambda=116.6$ nm as the mean free path of the inelastically scattered electrons.

Fig. 2 (a) shows a merged image of six BF-STEM images showing overall area of the wedge-shaped 4H-SiC specimen shown in Fig. 1(a).

These images were acquired with a two-beam condition exciting 11 $\overline{2}$ 0 reflection of the 4H-SiC as shown in Fig. 2(b). The specimen becomes thicker from the right to the left of the image. The specimen thickness is indicated below the image. Dislocations are seen as dark contrasts, and it is noteworthy that dislocations are observed even in the 5 μ m-thick area. This proves that 1 MeV electrons can transit through a 5 μ m-thick SiC crystal. This value is more than 50 times thicker than that used in conventional TEM.

Fig. 3(a) shows the thickness dependence of the width of dislocation images measured from the BF-STEM and BF-TEM images obtained at 1

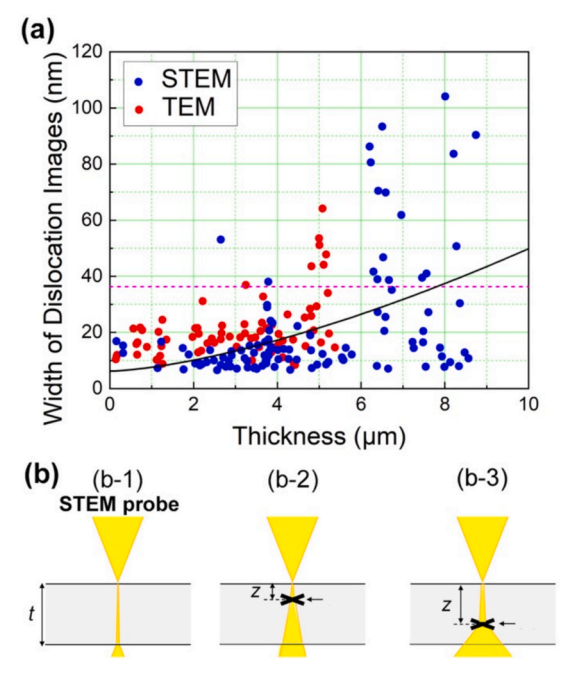


Fig. 3. (a) Thickness dependence of the width of dislocation images measured from BF-STEM and BF-TEM images (1 MV, $g=11\ \overline{2}$ 0). The solid curve represents fitting to the STEM results: $w=6.21+1.38t^{1.5}$. (b) Schematic diagram showing the propagation of STEM probe through a specimen and the top–bottom effect. (b-1) STEM probe spreads $\propto t^{1.5}$. (b-2) dislocation depth $z \ll t/2$. (b-3) $z \sim t$. The arrows in (b-2) and (b-3) indicate the positions of dislocations.

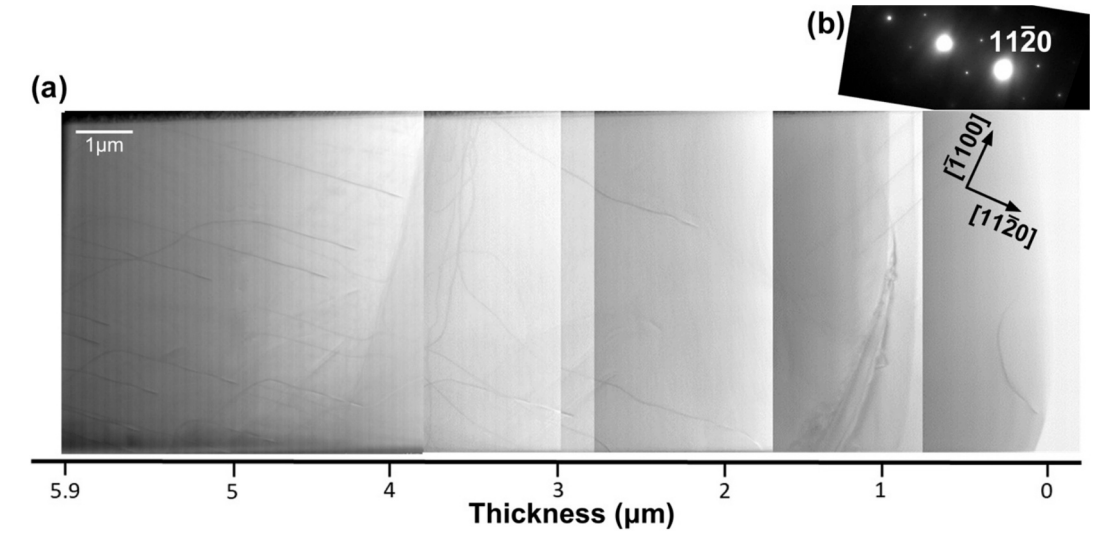


Fig. 2. (a) A merged BF-STEM image showing overall area of the wedge-shaped 4H-SiC specimen shown in Fig. 1(a). The image pixel size was 6.1 nm. (b) Selected area electron diffraction pattern with a two-beam condition exciting $11\ \overline{2}$ 0 reflection.

K. Sato et al. Materials Letters 402 (2026) 139310

MV. A total of three types of wedge-shaped specimens, including the specimen shown in Fig. 1(a), were used to measure these data (see Supplementary Fig. 2S). The excitation error (s_g) was set to slightly positive values: $s_g = 7 \times 10^{-3} \sim 1 \times 10^{-2} \text{ nm}^{-1} (1.2 \sim 1.3 \text{ g, g denotes the})$ Bragg reflection, i.e., $11\overline{2}$ 0). Under conditions where the s_g is slightly positive, intensity of BF images is effectively enhanced as indicated by the Darwin-Howie-Whelan equation [6]. The intensity profile measured in the direction perpendicular to the dislocation line in the image was fitted with the Lorentzian function, and the full width at half maximum of the fitted curve was defined as the width of dislocation image (see Supplementary Fig. 3S). As seen, width of dislocation image increases (namely, blurred) as the specimen thickness increases both for STEM and TEM. The broadening in TEM can be explained by blurring due to chromatic aberration caused by the increase in inelastically scattered electrons with increasing specimen thickness (see Supplementary Fig.4S). On the other hand, STEM is free from the effect of chromatic aberration arising from the imaging lens system, since it uses no imaging lens located after the specimen position. Therefore, the broadening in STEM can be mainly explained by the broadening of the STEM probe during its propagation through the specimen. A noteworthy result is that HVEM allows the visualization of dislocations in a 5 μ m-thick crystal with a spatial resolution of ~ 10 nm. Another major advantage of STEM is that scanning with converged electron probe virtually eliminates thickness fringes and bend contours arising from diffraction contrast [6], making it easier to observe dislocations [see Supplementary Fig.4S]. As a criterion for the observable thickness, an upper limit for the dislocation width was set at ξ_{hkl} / $\pi=36.3$ nm (horizontal dotted line in Fig. 3 (a)), below which dislocations were considered visible (ξ_{hkl} stands for the extinction distance of the hkl reflection excited for imaging, i.e., $11\overline{2}$ 0 in this study) [5]. The maximum observable thickness obtained was $8.6~\mu m$ for BF-STEM and $5.4~\mu m$ for BF-TEM both operating at 1 MV. This result can be compared with those obtained for GaN (6.9 µm [5]) and Si $(14.7 \, \mu m \, [7])$ in STEM mode using a similar method. In another study on Si, dislocations in 10 µm-thick specimens have been visualized using energy-filtered HVEM [8]. The material dependence of observable thickness can be attributed roughly to differences in mass thickness, i.e. density of materials (6.1, 3.2, and 2.3 g/cm³ for GaN, SiC, and Si, respectively). Although knock-on atom displacement is unavoidable at 1 MV, no obvious irradiation defects were observed that would prevent the observation of dislocations.

Spread of a STEM probe in a specimen is theoretically expressed as the 1.5th power of the specimen thickness (t) [6], which corresponds to the blurring of the width of dislocation image (w). The solid curve shown in Fig. 3(a) represents the fitted curve expressed as $w = 6.21 + 1.38 t^{1.5}$. However, in the region where the thickness exceeds 6 µm, the experimental results deviate significantly from the fitting curve. This is probably due to the top–bottom effect [6,9] caused by the depth (z: 0 < z < t) at which dislocations exist in the specimen. That is, when the dislocation is near the electron exit surface, the image will be blurred compared to when the dislocation is near the entrance surface, as shown schematically in Fig. 3(b). This is because in the former case the dislocations are scanned with a broadened electron probe. Multiple dislocations may exist close together, overlap in the projection direction, or intersect and become entangled. These may cause blurring of dislocation images regardless of the thickness. This scenario is plausible because the artificially introduced dislocations are thought to be non-uniformly

distributed around the crack. This is different from the case of threading dislocations introduced into GaN crystals during crystal growth, where the dislocation width can be roughly approximated by $t^{1.5}$ [5]. Further studies are needed to clarify the relationship between dislocation depth and visibility.

4. Conclusions

We have studied the observable thickness of the 4H-SiC crystals using HVEM operated at 1 MV. Based on the width of the dislocation images, it was demonstrated that the maximum thickness observable by BF-STEM (8.6 $\mu m)$ is superior to that by BF-TEM (5.4 $\mu m)$. BF-STEM is capable of visualizing dislocations contained in a specimen with thickness below $\sim 5~\mu m$ with a spatial resolution of $\sim 10~nm$. The method proposed in this study will be useful for defects-related failure analysis of electronic devices. A quantitative evaluation of the effect of dislocation depth on visibility remains a future challenge.

CRediT authorship contribution statement

Kazuhisa Sato: Writing – original draft, Methodology, Investigation, Formal analysis, Conceptualization. **Kotaro Hosono:** Investigation. **Shunya Takagi:** Investigation.

Declaration of competing interest

The authors declare that they have no known competing financial interests or personal relationships that could have appeared to influence the work reported in this paper.

Acknowledgments

The authors wish to thank Prof. J. Yamasaki of the University of Osaka and Dr. K. Asayama of JEOL Ltd. for invaluable comments. This study was partially supported by Grant-in-Aid for Transformative Research Area (A) (No. 21H05196) from the JSPS.

Appendix A. Supplementary data

Supplementary data to this article can be found online at https://doi. org/10.1016/j.matlet.2025.139310.

Data availability

Data will be made available on request.

References

- [1] T. Kimoto, H. Watanabe, Appl. Phys. Exp. 13 (2020) 120101.
- [2] T. Tanikawa, et al., Appl. Phys. Exp. 11 (2018) 031004.
- [3] K. Ishiji, et al., Jpn. J. Appl. Phys. 63 (2024) 12SP18.
- [4] H. Fujita, et al., Jpn. J. Appl. Phys. 6 (1967) 214–230.
 [5] K. Sato, H. Yasuda, ACS Omega 3 (2018) 13524–13529.
- [6] L. Reimer, Transmission Electron Microscopy, 3rd ed., Springer-Verlag, Berlin, Heidelberg, 1993.
- [7] K. Sato, et al., Jpn. J. Appl. Phys. 56 (2017) 100304.
- [8] S. Sadamatsu, et al., Ultramicrosc 162 (2016) 10–16.
- [9] H. Hashimoto, J. Appl. Phys. 35 (1964) 277–290.